ON THE ORIGIN OF CLUSTERS IN CENTRAL Au ON Au COLLISIONS AT SIS ENERGIES*

W. REISDORF

FOPI COLLABORATION

Gesellschaft für Schwerionenforschung mbH
D-6100 Darmstadt, Federal Republic of Germany

(Received September 20, 1993)

Au on Au collisions at 150, 250 and 400 A MeV were studied with a high granularity detector covering approximately the forward hemisphere in the center of mass. Methods to select and test centrality of collisions are described. A midrapidity source emitting clusters up to neon is found at all energies. An analysis with a quantum statistical model shows that the chemical composition of the source implies surprisingly low freezeout temperatures and entropies. The kinetic energy spectra of the emitted clusters are found to deviate considerably from Boltzmann–Maxwell distributions. Instead, they are compatible with a blast scenario, the energy stored in the blast exhausting about 50% of the available energy. It is suggested that the blast provides the mechanism necessary to understand the cooling and hence the observed clusterization. Consequences of the nuclear blast on other observables are discussed.

PACS numbers: 25.70. Pq, 25.75. +r

1. Introduction

The organization of this lecture is best described with use of a figure that I borrow from the diploma thesis of Peilert [1]. The figure shows the evolution with time (top to bottom) and impact parameter (left to right), as predicted by Quantum Molecular Dynamics (QMD) [2] for collisions of Au with Au at an incident energy of 200 A MeV. For impact parameters of 11 fm one finds after 200 fm/c a clear memory of the incident channel configuration: two large "fragments" are emerging. Going to 7 fm these

* Presented at the XXIII Mazurian Lakes Summer School on Nuclear Physics, Piaski, Poland, August 18–28, 1993.

projectile- and target-like fragments have become smaller and a new "intermediate object" now clearly shows up, which consists primarily of single nucleons. For impact parameters of 3 fm or less it is virtually impossible to identify any of the outgoing particles as being associated with the target or the projectile. Looking more closely at the $b = 1$ fm panels we notice that, at 40 fm/c a rather compressed almost spherical configuration has been formed, which at 200 fm/c has expanded considerably. The expanded object consists not only of single nucleons, but shows a tendency towards clusterization. We shall term this phenomenon "multi-clusterization" to distinguish it from "multifragmentation ".

The phenomenon which, as I will show, indeed exists, is remarkable, since the total energy available in the c.o.m. is $\approx$ 40 MeV/nucleon, while the typical binding energy for nuclei is 8 MeV/nucleon. Clusterization in expanding systems seems to exist on all scales and in particular we know from astrophysics that in the biggest of all scales available to us, one can see that even galaxies tend to clusterize [3].

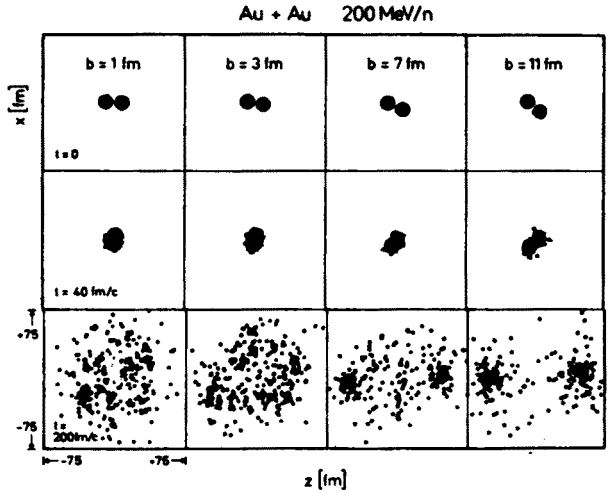

Fig. 1. Time development of a typical Au + Au collision for various impact parameters. After Peilert [1].

We shall be concerned with this expanding object (left-most panel in Fig. 1), which was called "nuclear big bang" by Andrzej Budzanowski [4]. First we will briefly describe the apparatus used and the methods that we developed to select central collisions. Then we shall look at the chemical composition of the outgoing particles and try to get a first estimate of the apparent temperature and entropy this composition implies at "freeze-out" time. We will then show that a nuclear "blast" is indeed observed by

analysing the velocities of these particles as a function of their mass. Finally, we will discuss the implication of this "expansion physics" on theory and on other observables.

2. Experimental method

Using the 4π detector FOPI [5] an exclusive experiment was performed at GSI-Darmstadt for the reaction Au on Au at 100, 150, 250, 400, 600 and 800 A MeV where all charged particles between $Z = 1$ and 15 were observed. We shall discuss here only the 150, 250 and 400 A MeV data.

The FOPI detector of phase I , shown in Fig. 2, consists of a high granularity time-of-flight wall (764 scintillators), supplemented with an inner shell of thin energy-loss detectors (188 elements) and a He-bag. Laboratory polar angles of $1° - 30°$ are covered over the full azimuth. The system allows element identification of particles ($Z \leq 15$) with detection thresholds increasing for $Z = 1$ to 15 from 14 to 50 A MeV respectively. About 10^6 events, or more, were collected at each incident energy, triggering on the charged particle multiplicity ($M_c > 10$) in the angular range $7° \leq \theta_{lab} \leq 30°$.

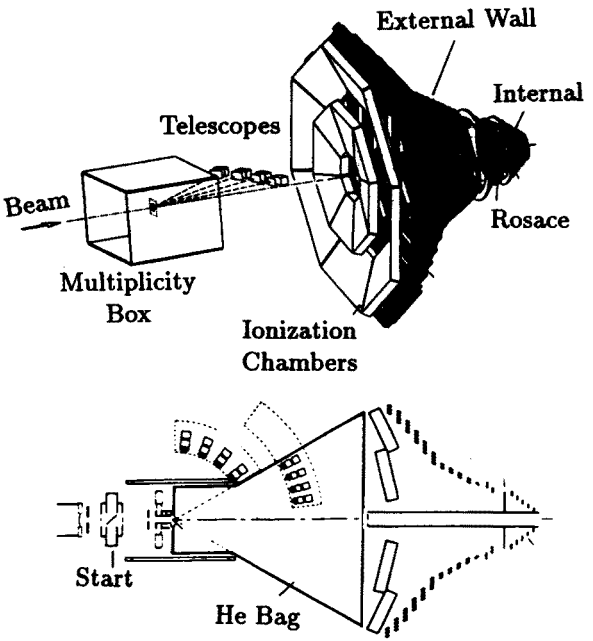

Fig. 2. Experimental Setup of the FOPI detector Phase I.

For completeness we note that in the phase II setup the multi-wire (multiplicity) chambers (see Fig. 2) have been replaced by a superconducting solenoid with associated drift tracking chambers, time-of-flight and

Cherenkov detectors. Experiments with this new setup (allowing to identify pions, as well as H and He isotopes) have already been performed, but will not be discussed here.

The selection of truly central collisions (say with impact parameter $b \leq 2$ fm) is not trivial since peripheral collisions are favoured by geometry. Traditionally, the measured charged-particle multiplicity has been used as a selection criterion. Intuitively, the most "violent" collisions are expected to have maximum centrality. For emerging fragments of charge 5 (boron) we show in Fig. 3 contour plots in the rapidity, y, versus specific transverse momentum, $p_t/mass$, plane. The most "central bin" of various observables has been selected [6]: *(i)* the charged particle multiplicity PM measured in the External Wall, (7° – 30°), *(ii)* the "participant" multiplicity PART-MUL, defined by excluding counts in the "projectile spectator area" (we are insensitive to target "spectators" in Phase I) and adding counts from the multiwire chambers (which see primarily mid-rapidity particles) *(iii)* the sum of observed charges ZMIDY in the midrapidity region, and finally *(iv)* the ratio of total observed transverse to longitudinal kinetic energies $E_\perp/E_\parallel$ (ERAT) in the forward hemisphere. In looking at these plots one has to be aware that the outermost contour is determined by the 30° laboratory cut for high p_t and by detector thresholds for negative rapidities. The outstanding feature is the appearance of a midrapidity source emitting high-mass (or charge) clusters, particularly strikingly in the ERAT binning.

The detailed topology, however, is seen to vary with the way "centrality" is defined. In particular the PM selection differs strongly from the other selections (all four selections correspond approximately to a 3 fm impact parameter cut in the sharp cutoff picture). QMD calculations including our apparatus cuts [6] strongly support that selection of high $E_\perp/E_\parallel$ (ERAT) values singles out the most central collisions.

Experimentally, this is corroborated by adding a second criterion for centrality: central collisions should be *axially symmetric* and in particular there should not be a sideways flow of particles [7]. Various observables can be defined to measure sideways flow and hence the non-axiality of the collision. The *directivity*, D [8, 9]

$$D = \frac{|\sum_i \vec{p}_{ti}|}{\sum_i |p_{ti}|}, \tag{1}$$

or the flow observable F' [10]

$$F' = \frac{(\sum_i \vec{p}_{ti})^2 - \sum_i p_{ti}^2}{(\sum_i A_i)^2 - \sum_i A_i^2}. \tag{2}$$

In both equations the sums are restricted to the forward hemisphere in the c.o.m.. The directivity is a dimensionless measure of the collinearity of the

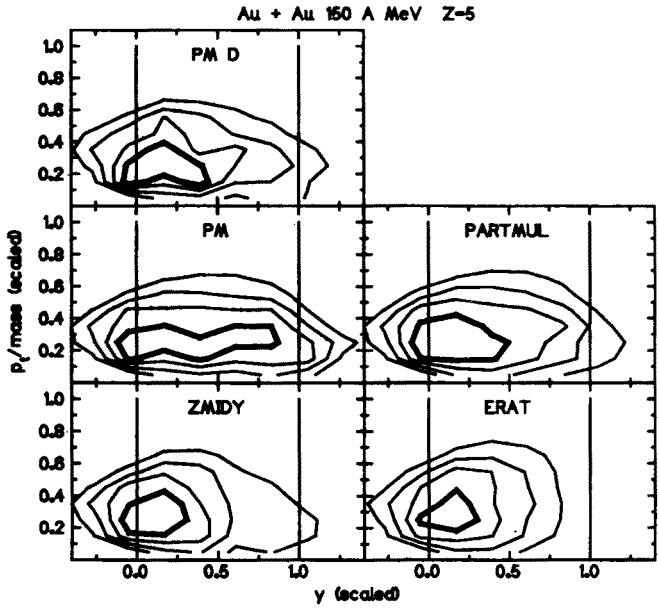

Fig. 3. Variation of the topology of the invariant cross sections $d^3\sigma/dyd^2p_t$ for boron ($Z = 5$) fragments according to various selection criteria explained in the text. The c.o.m. rapidity and the transverse momenta p_t have been scaled with the c.o.m. rapidity, resp. momentum of the projectile. The contours are on a linear scale separated by 20% intervals. The reaction is Au on Au at 150 A MeV.

various transverse momenta and converges to zero for axial symmetry in the limit of large multiplicities. The observable F' is zero on the average for axial symmetry. Under certain assumptions the square root of the related quantity [11] F_s

$$F_s = \frac{M_c}{M_c + 1} \frac{(\sum_i \vec{p}_{ti})^2 - \sum_i p_{ti}^2}{(\sum_i A_i)^2}, \tag{3}$$

can be interpreted as an absolute value for the *directed* transverse momentum.

Fig. 3 shows in the "PM D" panel that an additional cut on directivity ($D \leq 0.2$) makes the highest PM bin look much more like the other selections. Indeed, one can show [6, 11] that the ERAT bin has the lowest average values of D and F_s and hence is the most central selection. The behaviour of the important observable F_s will be discussed again later.

We conclude then at this stage that we have been able to isolate central collisions and find a *midrapidity* source emitting *clusters* as heavy as boron [9].

3. The chemical composition of the midrapidity source

At the incident energies discussed here, the available energies in the c.o.m. vary from about 37 to 95 Mev/nucleon which is much more than 8 MeV/nucleon, the average binding energy of cold nuclei. Nevertheless clusters with mass as high as 20 come out at midrapidity. Fig. 4 shows the measured Z-distribution for central collisions at 150, 250 and 400 A MeV. They are very well characterized by exponential slopes (solid lines), the steepness increasing with energy. Notice the only sizeable deviation from the trend is associated with $Z = 4$ (Be). This can be traced to the instability of ^{8}Be which decays into two alpha particles before it reaches the detectors.

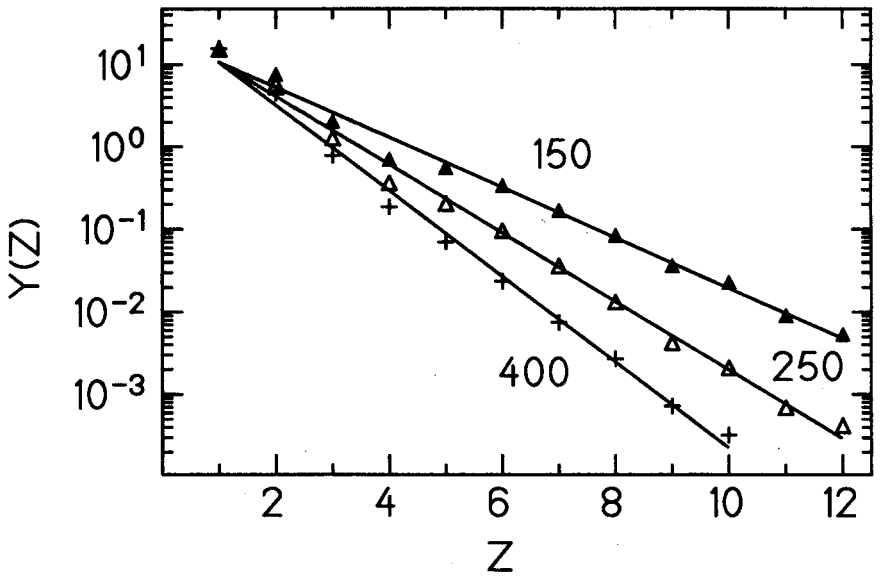

Fig. 4. The charge distribution for central collisions at 150, 250 and 400 A MeV. For 150 A MeV the data are normalized to the number of events, the data for 250 (400) A MeV have been rescaled by a factor 0.64 (0.49) in order to make the $Z = 1$ points coincide, which allows a better comparison of the slopes. The lines are exponential least-squares fits.

The figure also shows (take into account the scaling factors given in the caption) that it is rather arbitrary to judge the "rise and fall of multifragmentation" [12] or the "onset of vaporization" [13] just by looking at clusters with $Z > 2$. What we find is a *gradual* diminishing of the *size* of the clusters with incident energy. The special role alpha particles might play was speculated upon in ref. [30]. Calculations by Ono et al. [14] in the

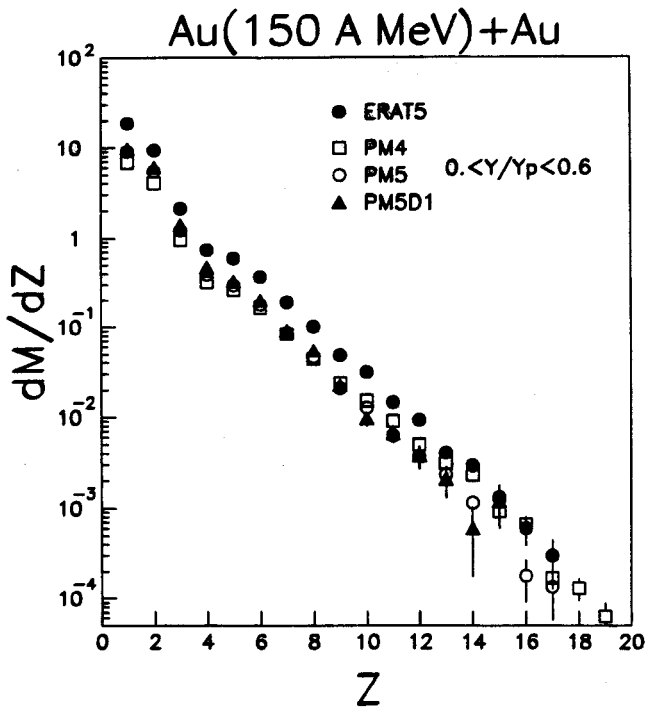

Fig. 5. Event-normalized charge distributions for various "participant" matter selection criterions (see also text): most central ERAT selection (ERAT5), highest multiplicity PM selection with directivity cut (PM5D1), multiplicity bins PM4 and PM5 with midrapidity cuts [12].

frame of antisymmetrized molecular dynamics clearly show the importance (shell effects !) of alphas.

Fig. 5 shows that at fixed beam energy the slope is characteristic of "participant" matter [15]: while this chemical soup is the dominating part in central collisions, one can also sort it out in less central collisions by applying midrapidity cuts. The conclusion is that to a first approximation, the chemical properties of the "fireball" depend only weakly on its size.

Clearly then, this observation leads one to consider equilibrium thermodynamics in a first effort to characterize the chemical composition of this "object ". Fig. 6 shows pairs of temperature-density points (T, ρ) implied by the Quantum Statistical Model (QSM) [16] if the experimental data in Figs 4 and 5 are to be reproduced. In the QSM a system of A nucleons is considered in the grand canonical ensemble. A large variety of about 600 stable and unstable fragment species with appropriate degeneracy, binding energy and quantum distribution function is considered and the thermodynamical properties of the resulting mixture are calculated. It is assumed

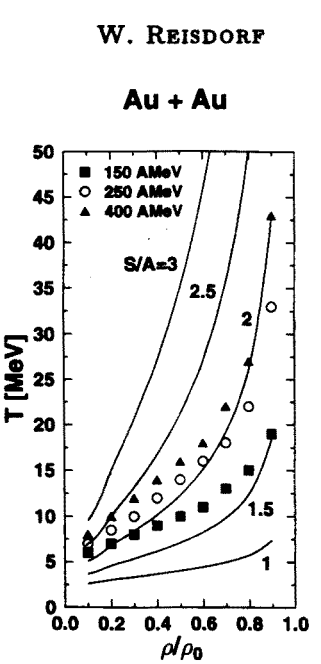

Fig. 6. Temperature versus freeze-out density (in units of ρ_0, the cold nuclear matter saturation density) for the Au on Au reaction at 150, 250 and 400 A MeV. The data points were obtained by comparing the experimental charge multiplicity distributions with those calculated with use of the Quantum Statistical Model [16]. Isentropes are also shown. From Ref. [12].

that thermal and chemical equilibrium are established during the expansion of the system. After freeze out the fragment yields change still due to the subsequent decay of unstable states. The chemical potential of a cluster in equilibrium is given by the chemical potential of its nucleon constituents and its binding energy. For the calculation of the thermal energy of each species the fragments are considered as hard spheres of fixed volume which move in the available free volume without mutual interactions.

One of the amazing outcomes of this study is that the apparent temperatures are very low. To be specific, at 400 A MeV one finds an apparent temperature of about 10 MeV at a realistic (see later) density $\rho/\rho_0 = 0.2$ (ρ_o is the cold nuclear matter saturation density). Using the ideal-gas formula, which should be roughly valid at sufficiently high temperatures, one would get $T \approx 50 - 60$ MeV for complete thermalization of an $E/A = 400$ MeV beam. How far one is away from this regime is also indicated by the low entropy values implied by the data: in Fig. 6 lines of constant entropy per nucleon (S/A) have been plotted: one finds S/A between 1.5 and 2.5 in this

energy regime. Looking at the Sackur–Tetrode equation for the ideal gas

$$\frac{S}{A} = 2.5 + \ln \frac{l_s^3}{\lambda_T^3}, \tag{4}$$

where $l_s^3 = V_s$ is the specific volume (volume per particle) and λ_T is the thermal wavelength

$$\lambda_T = \left(\frac{2\pi\hbar^2}{mT}\right)^{1/2}, \tag{5}$$

(m is the particle mass), we can convince ourselves that we are fully in the *quantum* statistical regime, since Eq. (4) holds only for $\lambda_T \ll l_s$, *i.e.* S/A values much larger than 2.5. The understanding of clusterization without quantum features in the theory is not possible. Note also that $T = 10$ MeV implies *local* cluster collisions in "low-energy" physics regime, *i.e.* predominantly fusion (clusterization) and deep inelastic collisions take place.

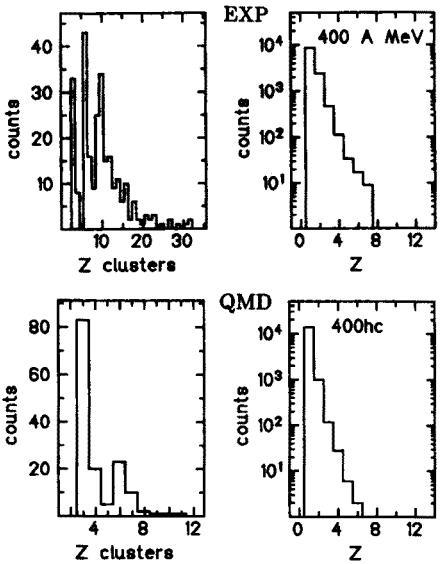

Fig. 7. Comparison of the experimental (upper panel) degree of clusterization with the predictions of (filtered) QMD using the hard equation of state at 400 A MeV. The left-hand panels describe the sum of charges per event due to clusters with charges higher than two.

But are statistical approaches justified? With this question in mind it seems imperative to apply a *dynamic* model to the problem. The QMD model which I shall use has already been described thoroughly by Budzanowski at this School, so I can limit myself to showing results using the

model [2]. Concerning the chemical composition predicted by the model one can say that it describes our data at 150 A MeV fairly well, but as can be seen in Fig. 7, it strongly underestimates clusterization at 400 A MeV. The version [2] we have used does not consider the late deexcitation of the excited clusters, so the predictions probably even *overestimate* the number of surviving clusters. A more recent development [17] of the model that uses a semiclassical Pauli potential to simulate Fermi motion seems to confirm the high degree of excitation of the clusters at freeze out, thus making it very difficult to explain our experimental data at the present time on the basis of dynamical theories. Clearly more experimental guidance (from other observables) is needed.

4. Kinetics: an exploding source

Fig. 8 shows c.o.m. kinetic energy spectra of the clusters emerging from central collisions at 150 A MeV. If one compares these spectra [18] with the expectations from a purely thermal model (modified version of FREESCO) [19], one sees a spectacular discrepancy when looking at heavier and heavier clusters: the spectra are considerably harder than inferred on the basis of the hydrogen spectrum. We note that the purely thermal scenario included the influence of Coulomb repulsion after freeze out (at $\rho/\rho_0 = 0.3$).

One can try to understand or at least parameterize these observations by assuming that the midrapidity source *explodes* under the influence of (shock?) compression [20] and/or heat [21, 22]. This nuclear "blast" can be characterized by a radial outward flow common to all particles. Following Refs [21, 22] we can make a simple Ansatz for the velocity distribution resulting from a superposition of (ordered) flow, characterized by a flow velocity v_f, and (disordered) thermal motion characterized by a "local" temperature T

$$dN(\vec{v}) = \frac{mvdv}{\pi^{1/2}T}\left(\frac{mv_f^2}{2T}\right)^{-1/2} \exp\left(-\frac{mv_f^2 + mv^2}{2T}\right) \sinh\left(\frac{mv_f v}{T}\right). \quad (6)$$

Hydrodynamics (notably the mass-continuity equation) suggests that a *distribution* of flow velocities will have developed at freeze-out time, such that v_f will be approximately proportional to the c.o.m. distance of the particles at freeze-out, which would correspond to the "red-shift" in astrophysics. (more complex distributions are predicted in specific models [20, 21, 23–25]).

We have explored both the single (or average) flow velocity and the "redshift" or "hydrodynamics" scenarios. Fig. 8 shows calculations (solid histograms) in the redshift scenario using again FREESCO: although the data are not reproduced in finer details, one can see that a total radial flow

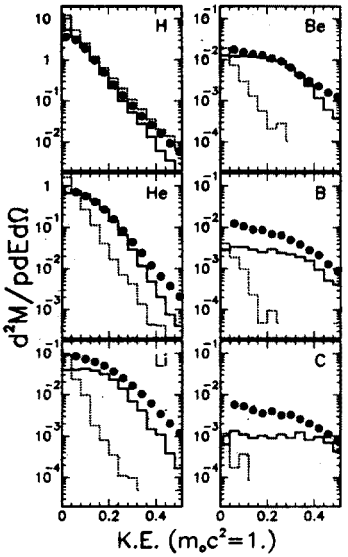

Fig. 8. Kinetic energy spectra of clusters ($Z = 1 - 6$) emitted in central collisions under $(25 - 45)^\circ$ in the c.o.m. at incident energy of 150 A MeV. The dotted histograms are from calculations from a purely thermal scenario, for the solid histograms a radial blast of 18 A MeV has been superimposed on thermal motion conserving energy. From Ref. [18].

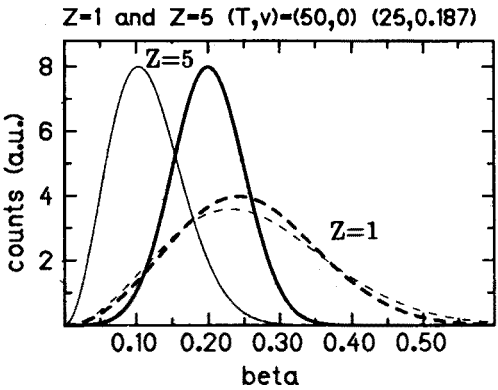

Fig. 9. Theoretical velocity spectra (count rates) for $Z = 1$ and 5 particles emitted in a purely thermal (thin lines, $T = 50$ MeV) and, alternatively, in a blast scenario ($T = 25$ MeV, $v_f/c = 0.187$).

of 18 MeV/u (!) superimposed on local thermal motion (conserving energy) goes a long way into the direction of explaining the data.

Nuclear blasts of the violence implied by the data change the velocities of heavy clustered products considerably, while the lighter particles

are hardly affected. This is shown in the lowest panel of Fig. 8 where the theoretical spectra of $Z = 1$ ($A = 2$) and $Z = 5$ ($A = 10$) particles are compared: The thinner lines hold for a temperature of 50 MeV without flow, the thick lines are for a flow scenario leading to a lower temperature of 25 MeV and a finite flow of $v_f/c = 0.187$). I have intentionally plotted *count rate* spectra rather than phase-space-density spectra to make a plausibility argument for the application of *likelihood* methods (that can be applied to *single* events): It is intuitively clear that if we observe in a *single* event, say thirty $Z = 1$ particles compatible with a quasithermal distribution (see the H-panel in Fig. 8) and, if in addition we see two or three heavy clusters with a velocity $v/c \approx 0.2$ (see Fig. 9), then *it is very unlikely that the purely thermal scenario (no flow) is the correct one.*

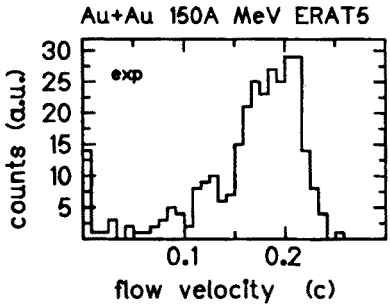

Fig. 10. Experimental radial flow velocity distribution of 300 central events in the reaction Au on Au at 150 A MeV.

This is confirmed by the actual analysis. Fig. 10 shows the distribution of average flow velocities, deduced from single-event analysis using likelihood methods [26] with full account of apparatus cuts. The 300 events analysed (Au on Au at 150 A MeV, central ERAT bin) show a clear peak at $v_f/c \approx 0.2$, the width of the peak being roughly 20%. Simulations show that the shape of the distribution is dominated by purely *statistical* fluctuations. As a consequence, superposition of events to a "macro" blast leads to a narrowing of the flow velocity uncertainty roughly with the square root of the number of superposed events. Thus a handful (10!) of events determine the radial flow velocity with a 6% accuracy already. The enormous power of likelihood methods allows 1) to do this analysis under extremely exclusive conditions 2) to apply it to sophisticated theories that generate only few events due to computer time limitations.

Fig. 10 also makes an important physics point, however: the radial blast is a feature of *single* events, not the result of a superposition of many *different* events leading to seemingly complex, perhaps multi-temperature, spectra. In Fig. 11 I show that various global observables (not Z separated,

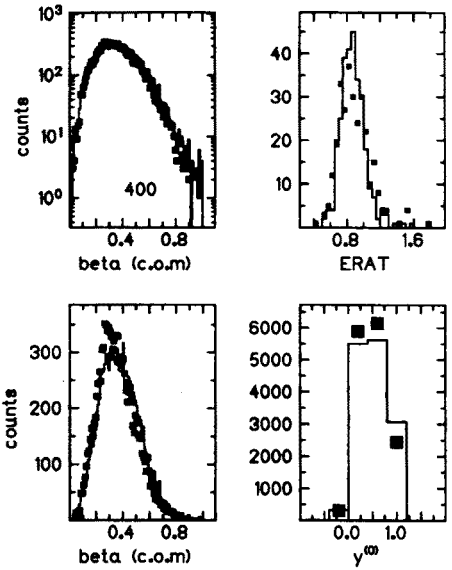

Fig. 11. Comparison of various experimental spectra (histograms), obtained for Au + Au at 400 A MeV by superposing 300 central events, with a simulation using the redshift blast scenario. The one parameter of the simulation was adjusted by single event analyses using likelihood methods. The left panels compare on a log as well as a linear scale the nuclear-charge weighted c.o.m. velocity spectra cumulated for all the particles over the full apparatus acceptance. The upper right panel considers the distribution of $E_\perp/E_\parallel$, the lower right panel the nuclear-charge weighted rapidity distribution. A radial flow of 42 A MeV was deduced. The *purely statistical* error (for 300 events) is 1 A MeV.

all influenced by apparatus cuts) are well reproduced by the likelihood fits, for example, to the 400 A MeV data. A radial flow energy of 42 A MeV (!) was deduced. The redshift scenario was used. Let me note that the tails of the $E_\perp/E_\parallel$ (ERAT) distribution are also reproduced, implying that they are also of purely statistical nature. A more refined comparison of Z and angle-separated spectra is in progress. I also note that I leave open, for the time being, the important question whether the blast has shock-like features leading to preferred 90° emissions for central collisions. (In our fits we did not require isotropy, but have assumed that the velocity distribution does not change with angle).

The extracted behaviour of radial flow at 150, 250 and 400 A MeV is summarized in Fig. 12. One has to realize from these results that approximately 50% of the available energy is seen in the form of ordered radial flow. This flow is more than an order-of-magnitude larger than known sideways flows ([7], see also our Fig. 14).

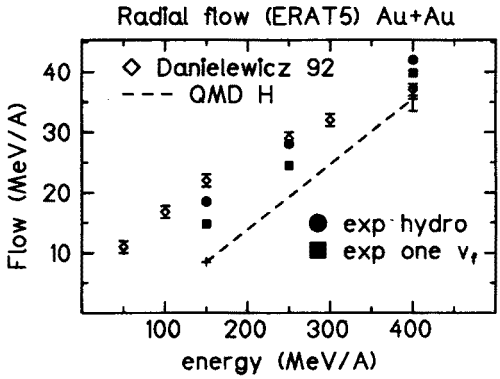

Fig. 12. Radial flow in central collisions of Au on Au. Experimental values are extracted with the likelihood method in the single flow velocity scenario (squares) and the redshift or hydrodynamics scenario (circles). The dashed line joins values extracted from QMD [2] events at 150 and 400 A MeV (hard EOS, redshift parameterization), the predictions of Danielewicz and Pan [27] are represented by diamond symbols.

In Fig. 12 I also compare with predictions from QMD [2] (using the hard equation of state EOS) and with the predictions of a transport theory for clusters up to mass three [27]. Concerning QMD, I have applied exactly the same apparatus-filtered single-event analysis (redshift scenario) to the "theoretical" events. One finds, for this particular QMD version, a strong underestimation (by a factor 2) of the radial flow at 150 A MeV, while a better agreement is found at 400 A MeV (where however, see Fig. 7, the model has difficulties reproducing the degree of clusterization). Concerning the model of Danielewicz and Pan [27] I have plotted half the difference of the calculated average kinetic energies of ^{3}He and protons at 90° (c.o.m.). The predictions are encouragingly close to our redshift-scenario results.

5. Consequences of the nuclear blast

What can we say at this stage? We have characterized central collisions by essentially two parameters: an (exponential) slope parameter for the degree of clusterization and a radial flow parameter. This "simplifies" the situation a lot, but also puts a stress on our theoretical understanding: *both* features must be reproduced by *one* theory.

The radial flow values deduced from the data, in particular the 42 A MeV flow of the 400 A MeV data completely exclude the hypothesis of a simple Coulomb explosion. The particles blast apart at one third of the light velocity. Are we witnessing the quasi-elastic release of nuclear compression energy, in other words, are we finally getting a handle on the nuclear equation of state (EOS)? At the present time we do not have a generally accepted

and sufficiently direct method to *measure* the maximum compression (mass and energy density) achieved in central heavy ion collisions. We therefore have to rely, still, on theoretical works. From the various calculations available in the literature (see for example [2, 25, 27]) one can conclude that compression energies much larger than 10 A MeV are predicted to be unlikely for incident energies not exceeding 400 A MeV. The influence of the EOS on this prediction seems to be rather modest. Another result from theory (cascade modelling [30] or hydrodynamics modelling [25]) might be more relevant in our context: the expansion phase is found to be rather isoentropic. There are two extremes where isoentropic expansion is fulfilled: 1) the collisionless mean-field driven expansion and 2) the relatively slow expansion during which thermal equilibration by interparticle collisions can keep up at all times (zero viscosity). In the latter case transformation of internal energy to a macroscopic outward flow will take place [31, 32], a "blast" develops and the local temperature will decrease during the expansion. As a consequence, nucleons will clusterize. A very rough plausibility argument can be made using the ideal monoatomic gas: along an isentrope $VT^{3/2}$ is constant, *i.e.* an expansion from $2\rho_o$ to $0.1\rho_o$ implies a cooling by a factor of 7. As simple as these arguments are, we still are far from a detailed understanding.

The possible isoentropic features of expansion need to be explored in dynamical microscopic models including also the mean field and true quantum features. Whatever the outcome, three time scales must be considered in order to make predictions about clusterization [32]: the typical expansion time, the equilibration time (which varies with density of course) and the "instability time ", *i.e.* the time needed, if regions of negative pressure gradients are reached, to form clusters. In 1984 Cugnon [32] estimated that both the equilibration times (about 10 fm/c) and the instability times (about 20 fm/c) might be short enough compared to the expansion time (about 60 fm/c) to allow a gas-to-droplet transition. In view of the violence of the blast found by our collaboration, these numbers must be regarded with caution. We are just at the beginning of our understanding of the clusterization phenomena and the blast development. It seems clear however that both aspects are correlated: *the blast is the key to the cooling mechanism needed to form clusters.*

Finally, let me stress that the blast phenomenon should influence many other observables. First of all, the macroscopic energy stored in the radial flow should massively influence particle creation (pions) and perhaps the "late" gamma spectra as well. Two other consequences concern two-particle correlations and sideways flow.

Fig. 13 shows measured [33] two-particle correlation functions for fragment pairs with nuclear charge ≥ 3 at an incident energy of 150 A MeV. In

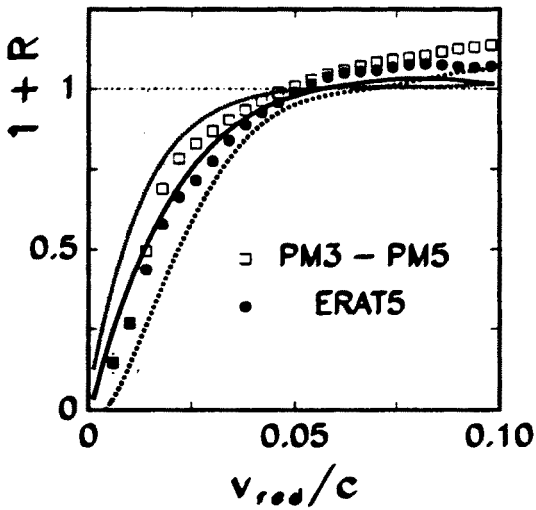

Fig. 13. Two-particle correlation function of fragments with nuclear charge ≥ 3 (most central ERAT bin, full circles, reactions with External Wall multiplicities > 19, squares). The smooth curves are calculations assuming freezeout radii of 10, 20 and 40 fm. The reaction is Au on Au at 150 A MeV. From Ref. [33].

these Coulomb-dominated cases, the correlations for differently sized fragments scale well [34] with the reduced relative velocity

$$v_{\rm red} = \frac{v_{12}}{\sqrt{Z_1 + Z_2}}, \tag{7}$$

where Z_1 and Z_2 are the fragment charges. From simulations [33] including the experimentally determined blast parameters (flow velocity and temperature) a most probable freezeout radius of 14 ± 2 fm could be deduced corresponding to $\rho = 0.2\rho_o$. Had the blast been ignored, a source half the size would have been predicted! The deduced density at freezeout can be used to fix the freezeout temperature (Fig. 6) in the framework of statistical models as discussed earlier.

In Fig. 14 I show the maximal measured sideways flow [11], the square root of the variable Eq. (3), in the energy range discussed here. To compare with the *radial* flow we have converted the momentum values to energies per nucleon. Again, we compare with QMD calculations using the hard EOS (for more detailed comparisons see [11]). It seems clear that the expanding hot participant soup will in part blast into the spectators causing these to absorb some of the heat (a mechanism not taken into account in most fragmentation models for spectator matter) and in addition to recoil sideways. Comparison of Figs 14 and 12 suggests that theories that underestimate

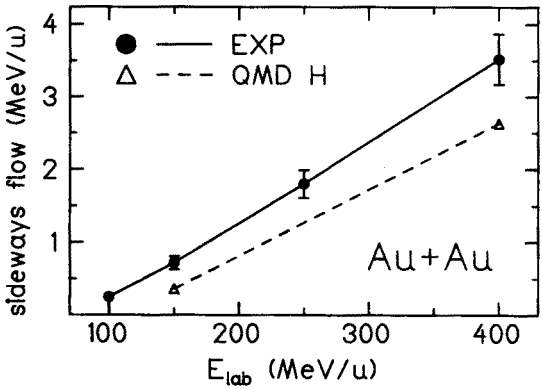

Fig. 14. Maximal sideways flow as a function of incident energy . QMD calculations at 150 and 400 A MeV (triangles) are compared with experimental data for the hard equation of state. After [11].

the radial flow are likely to underestimate the sideways flow as well: both kinds of flow are correlated. The sideways flow is more than an order of magnitude smaller than the radial flow, however. The "spectator" acts like a "nearby" calorimeter and recoil detector. Due to its "location" in a plane its "geometric efficiency" is small.

REFERENCES

[1] G. Peilert, *Diploma Thesis* , Johann Wolfgang Goethe-Universität Frankfurt, Frankfurt 1988.

[2] J. Aichelin, G. Peilert, A. Bohnet, A. Rosenhauer, H. Stöcker, W. Greiner, *Phys. Rev.* **C37**, 2451 (1988); G. Peilert, H. Stöcker, W. Greiner, A. Rosenhauer, A. Bohnet, A. Aichelin, *Phys. Rev.* **C39**, 1402 (1989).

[3] P.H. Coleman, L. Pietronero, *Phys. Rep.* **213**, 311 (1992).

[4] A. Budzanowski, *see these Proceedings*!?!!!?

[5] A. Gobbi *et al.*, *Nucl. Inst. Meth.* **A324**, 156 (1993).

[6] W. Reisdorf (FOPI collaboration), *Proc. XXth Int. Workshop on Gross Properties of Nuclei and Nuclear Excitation*, Hirschegg, Austria (1992), p. 38.

[7] H. A. Gustafsson *et al.*, *Phys. Rev. Lett.* **52**, 1590 (1984); *Mod. Phys. Lett.* **A3**, 1323 (1988); M. Demoulins *et al.*, *Phys. Lett.* **B241**, 476 (1990).

[8] P. Beckmann *et al.*, *Mod. Phys. Lett.* **A52**, 163 (1987).

[9] J.P. Alard *et al.*, *Phys. Rev. Lett.* **69**, 889 (1992).

[10] P. Danielewicz, G. Odyniec, *Phys. Lett.* **B157**, 146 (1985).

[11] T. Wienold, Doctoral Thesis , Universität Heidelberg, Heidelberg 1993.

[12] C. A. Ogilvie *et al.*, *Phys. Rev. Lett.* **62**, 1214 (1991).

[13] M.B. Tsang *et al.*, *Phys. Rev. Lett.* **71**, 1502 (1993).

[14] A. Ono, H. Horiuchi, T. Maruyama, A. Onishi, *Phys. Rev. Lett.* **68**, 2898 (1992).

[15] C. Kuhn, J. Konopka, J.P. Coffin *et al.*, *Phys. Rev.* **C**, in press (1993).
[16] D. Hahn, H. Stöcker, *Phys. Rev.* **C37**, 1048 (1988).
[17] G. Peilert, J. Randrup, H. Stöcker, W. Greiner *Phys. Lett.* **B260**, 271 (1991); G. Peilert, J. Konopka, H. Stöcker, W. Greiner, M. Blann, M. G. Mustafa, *Phys. Rev.* **C46**, 1457 (1992).
[18] S.C. Jeong, N. Herrmann, J. Randrup *et al.*, GSI preprint, GSI-93-38 (1993).
[19] J. Randrup, G. Fai, *Phys. Lett.* **B115**, 281 (1982); J. Randrup, LBL preprint 33865 (1993).(accepted by *Comp. Phys. Comm.*).
[20] W. Scheid, H. Müller, W. Greiner, *Phys. Rev. Lett.* **32**, 741 (1974).
[21] J.P. Bondorf, S.I.A. Garpman, J. Zimany, *Nucl. Phys.* **A296**, 320 (1978).
[22] P.J. Siemens, J.O. Rasmussen, *Phys. Rev. Lett.* **A42**, 880 (1979).
[23] H. Stöcker *et al.*, *Phys. Rev. Lett.* **44**, 725 (1980); *Phys. Rev.* **C25**, 1873 (1982).
[24] G. Buchwald, G. Graebner, J. Theis, J. Maruhn, W.Greiner, H. Stöcker, *Phys. Rev. Lett.* **52**, 1594 (1984).
[25] W. Schmidt, U. Katscher, B. Walhauser, J.A. Maruhn, H. Stöcker, W. Greiner, *Phys. Rev.* **C47**, 2782 (1993).
[26] W. Ledermann, *Handbook of Applicable Mathematics, Volume VI: Statistics*, John Wiley and Sons, Chichester, New York 1984.
[27] P. Danielewicz, Qiubao Pan, *Phys. Rev.* **C46**, 2002 (1992).
[28] A. Lang, B. Blättel, W. Cassing, V. Koch, U. Mosel, K. Weber, *Z. Phys.* **A340**, 287 (1991).
[29] D.T. Khoa, N. Ohtsuka, M.A. Matin, A. Faessler, S.W. Huang, E. Lehmann, R.K. Puri, *Nucl. Phys.* **A548**, 102 (1992).
[30] G. Bertsch, J. Cugnon, *Phys. Rev.* **C24**, 2514 (1981).
[31] G. Bertsch, P.J. Siemens, *Phys. Lett.* **B126**, 9 (1983).
[32] J. Cugnon, *Phys. Lett.* **B135**, 374 (1984).
[33] B. Kämpfer, R. Kotte *et al.*, preprint Rossendorf FZR-93-14, accepted by *Phys. Rev.* (1993).
[34] Y.D. Kim, R.T. de Souza, C.K. Gelbke, W.G. Gong, S. Pratt, *Phys. Rev.* **C45**, 387 (1992).